

Structural and catalytic properties of alkyl-substituted phosphanes.

Effect of *ortho*-modification on rhodium-catalyzed 1-hexene hydroformylation

Pekka Suomalainen^a, Helena Riihimäki^b, Sirpa Jääskeläinen^a, Matti Haukka^a, Jouni T. Pursiainen^b
and Tapani A. Pakkanen^a

^a Department of Chemistry, University of Joensuu, PO Box 111, FIN-80101 Joensuu, Finland

^b Department of Chemistry, University of Oulu, PO Box 3000, FIN-90401 Oulu, Finland

Received 8 March 2001; accepted 2 August 2001

The influence of the alkyl-substituted phosphanes (*o*-methylphenyl)diphenylphosphane (*o*-MeP), (*o*-ethylphenyl)diphenylphosphane (*o*-EtP), bis(*o*-methylphenyl)phenylphosphane (*o*-Me₂P), bis(*o*-ethylphenyl)phenylphosphane (*o*-Et₂P), and (2,4,5-trimethylphenyl)diphenylphosphane (2,4,5-MeP) was screened in model reaction of rhodium-catalyzed 1-hexene hydroformylation. Compared with PPh₃, the prepared phosphanes afforded lower chemoselectivity towards aldehydes, but increased the normal to branched ratio. Catalyst results are discussed in relation to stereoelectronic properties of the phosphane ligands. Electron donor capacity of the ligands was studied in terms of spectroscopic data of the *trans*-RhCl(CO)P₂ species, formed in reaction between Rh₂(μ-Cl)₂(CO)₄ and the ligands (P). Furthermore, steric attributes of free and bound phosphanes were investigated by Tolmans cone angle method. Crystal structures for ligands *o*-EtP, *o*-Me₂P, *o*-Et₂P, and complexes *trans*-Rh(CO)Cl(*o*-MeP)₂ and *trans*-Rh(CO)Cl(*o*-EtP)₂ were solved as well.

KEY WORDS: rhodium; phosphane ligands; 1-hexene hydroformylation

1. Introduction

Tertiary phosphorus ligands are commonly used to enhance catalyst stability as well as chemo- and regioselectivity of the rhodium-catalyzed hydroformylation reaction [1,2]. Both the steric and electronic characteristics of the ligands affect the interaction between the catalyst and the substrate, and thereby the rate and the selectivity of the reaction [3]. A large number of different methods are available to study the stereoelectronic properties of phosphorus ligands and aid in the development of more efficient catalysts. For the estimation of steric properties of the ligands, Tolman's [4] cone angle concept and Casey's natural biting angle [5] have been widely utilized. For evaluation of the electronic character, Tolman's method based on the correlation of IR frequencies [6] with a plethora of other parameters, including ionization potential [7], half neutralization potential (HNP) [8], and ¹⁰³Rh chemical shifts [9] has been used.

The current paper reports structural studies on a set of closely related monodentate phosphanes: namely triphenylphosphane-type ligands modified with alkyl groups –CH₃ or –CH₂CH₃ in the *ortho* positions of the phenyl ring(s). We wished to know whether such small changes in the ligand structure could have an effect on the catalytic behavior. Previously, modification of triphenylphosphane ligands in the *para* position has been observed to have a substantial effect on activity and selectivity in hydrogenation [10] and hydroformylation [11].

The stereoelectronic effects of the ligands were studied by synthesizing a series of *trans*-Rh(CO)ClP₂ complexes in a reaction between Rh₂(μ-Cl)₂(CO)₄ and the ligands. Spectroscopic, crystallographic, and theoretical studies were employed to reveal the geometric and electronic interactions of ligands around the rhodium. We previously carried out cone angle calculations for gas-phase conformers [12]. The current paper extends the structural determinations for free and bonded solid-state geometries of the ligands.

The effect of *ortho*-modification was tested in rhodium-catalyzed 1-hexene hydroformylation reaction. Rh₄(CO)₁₂ was chosen as catalytic precursor as it does not contain any "interfering" ligands capable of competing with the *in situ* added alkyl-substituted phosphanes.

2. Results and discussion

2.1. Synthesis and properties of free ligands

The phosphane ligands (*o*-methylphenyl)diphenylphosphane (*o*-MeP) (**1**), (*o*-ethylphenyl)diphenylphosphane (*o*-EtP) (**2**), bis(*o*-methylphenyl)phenylphosphane (*o*-Me₂P) (**3**), and bis(*o*-ethylphenyl)phenylphosphane (*o*-Et₂P) (**4**) were prepared by a modified literature method [13] from brominated organic reagent by lithiation with *n*-butyl lithium and from halogenated arylphosphanes. In addition, a new ligand (2,4,5-trimethylphenyl)diphenylphosphane (2,4,5-MeP) (**5**) was synthesized. The ligands are presented in figure 1.

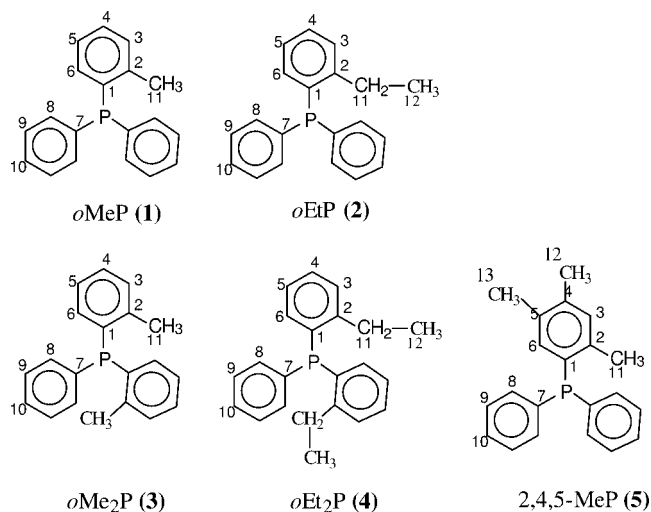


Figure 1. Schematic structures of the reported ligands; numbering corresponds to the NMR data.

Table 1
Spectroscopic data for the free and co-ordinated ligands.

Ligand (P)	Free P	Rh(CO)ClP ₂		
	³¹ P-NMR	³¹ P-NMR		IR ν(CO)
	σ (ppm)	σ (ppm)	¹ J _{P-Rh} (Hz)	(cm ⁻¹)
<i>o</i> -Et ₂ P	-23.5	23.3	123	1973
<i>o</i> -Me ₂ P	-19.0	23.6	125	1974
2,4,5-MeP	-11.8	24.9	124	1973
<i>o</i> -EtP	-14.2	25.4	127	1975
<i>o</i> -MeP	-10.7	25.8	125	1975
PPh ₃	-3.3	29.2	127	1978

Table 2
Cone angles for free and bound phosphanes.

Ligand (P)	Free ligand (X-ray)	Free ligand (HF-3-21G*)	Coordinated ligands (X-ray) Rh(CO)Cl(P) ₂
<i>o</i> -MeP	—	151°	159°
<i>o</i> -Me ₂ P	173°	158°	—
<i>o</i> -EtP	181°	169°	—
<i>o</i> -Et ₂ P	178°	194°	178°
2,4,5-MeP	—	159°	—

The phosphanes are air-sensitive, both as pure compounds and in solution, and therefore must be prepared and handled under a nitrogen or argon atmosphere. The ligands were recrystallized from ethanol, except for *o*-EtP, which was not recrystallized and was isolated as viscous oil. Single crystals for X-ray crystallographic analysis were obtained by slow evaporation of the dichloromethane–hexane solvent mixture at room temperature.

Steric demands for ligands are presented in table 2. As expected, the cone angle increased steadily with the degree of substitution of the ligand, from 151° for *o*-MeP to 194° for *o*-Et₂P. Deviations to the size of corresponding solid-state structures, due to crystal packing were observed. Electronically the ligands should not differ much from each other

or from triphenylphosphane (PPh₃). The role of such non-coordinating alkyl groups in catalysis may be to act as steering “arms” for the substrate, thus affecting the conversion and product distribution.

2.2. Rh complexes

Reaction between equimolar amounts of Rh₂(μ-Cl)₂(CO)₄ and alkyl-substituted phosphanes afforded rhodium complexes with the general formula *trans*-Rh(CO)ClP₂. Yellow compounds of *trans*-Rh(CO)Cl(*o*-MeP)₂ (**6**), *trans*-Rh(CO)Cl(*o*-EtP)₂ (**7**), *trans*-Rh(CO)Cl(*o*-Me₂P)₂ (**8**), *trans*-Rh(CO)Cl(*o*-Et₂P)₂ (**9**), and *trans*-Rh(CO)Cl(2,4,5-MeP)₂ (**10**) were isolated. Crystals for X-ray studies were grown from CH₂Cl₂/hexane solution. The similar stereochemistry of the complexes established comparable Rh(I) environment facilitating study of the stereoelectronic properties of the ligands around the metal sphere, and clarification of the catalytic behavior of the ligands in the hydroformylation of 1-hexene. The complex of *trans*-Rh(CO)Cl(PPh₃)₂ was prepared for comparison.

2.3. Spectroscopic characterization of Rh(I) complexes

Table 1 summarizes the ³¹P-NMR and FTIR data for the free and co-ordinated ligands. The coupling constant, ¹J_{P-M}, is a useful parameter for estimating the electron donor/acceptor properties of the co-ordinated ligands as it describes the property of a particular P–M bond [14]. Similarly, the carbonyl stretching frequency is (relatively) free of steric effects and thus reflects the electronic state of the bound phosphane ligand [4,15].

The narrow range of obtained IR stretching frequencies (1973–1975 cm⁻¹) and coupling constants (123–127 Hz) for *trans*-Rh(CO)Cl(P)₂ species suggests that the ligands are electronically similar. Further, the higher value of ν(CO) for *trans*-Rh(CO)Cl(PPh₃)₂ (1978 cm⁻¹) indicates greater basicity of the prepared phosphanes relative to PPh₃. Sigma donation from phosphorus ligands is known to increase the electron density at metal (rhodium) center, thus increasing the π-back-donation to the CO ligand and causing a decrease in the CO stretching frequencies. Further ranking of the ligands by their electron-donor–acceptor properties is not possible because of similarity of the spectroscopic data.

2.4. Structural characteristics of free and bound phosphanes

Complex **6** (figure 2) has a slightly distorted square planar structure, with greatest discrepancy along the axis C(25)–Rh(1)–Cl(1) with angle of 174.2°(2). Also the P–Rh–P angle 175.2°(5) deviates from the ideal, pointing to somewhat tetrahedral geometry about the rhodium atom. Further in complex **6**, the substituted phenyl rings were on the same side of the P–Rh–P axis, with methyl groups directed towards the rhodium atom. The cone angle for the co-ordinated *o*-MeP (159°) was in the same range to that of

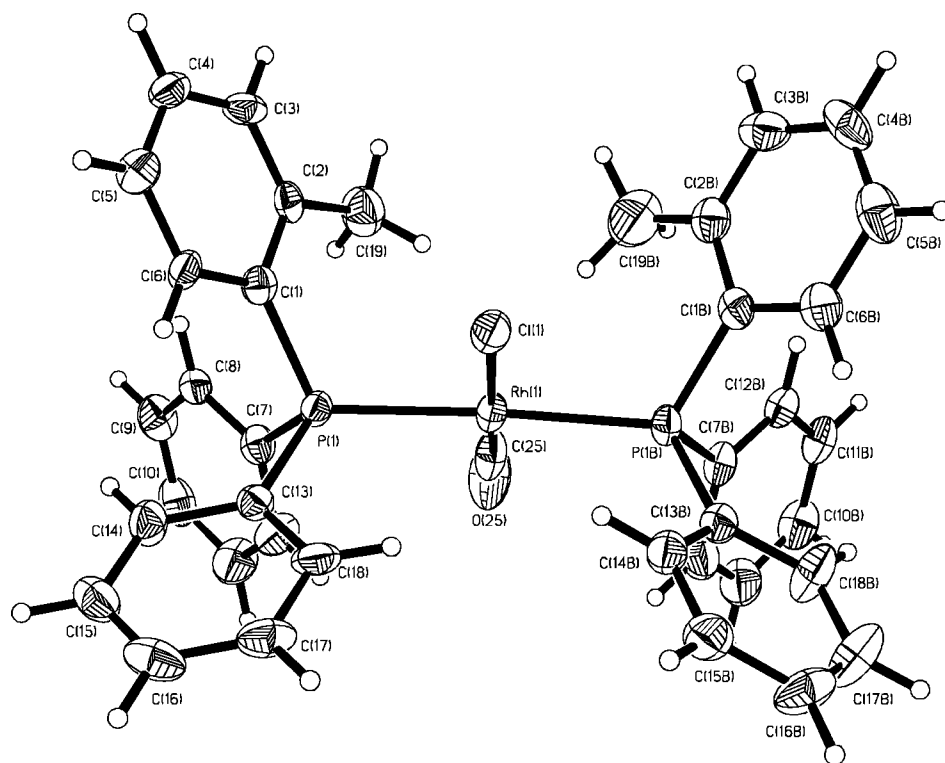


Figure 2. Ortep drawing of $\text{Rh}(\text{CO})\text{Cl}(\text{o-MeP})_2$ (**6**) with thermal ellipsoids at 50% level. Selected bond angles ($^\circ$) and distances (\AA): $\text{Rh}(1)\text{--C}(25)$ 1.808(6), $\text{Rh}(1)\text{--Cl}(1)$ 2.381(1), $\text{Rh}(1)\text{--P}(1)$ 2.328(1), $\text{Rh}(1)\text{--P}(1\text{B})$ 2.381(1), $\text{P}(1\text{B})\text{--Rh}(1)\text{--P}(1)$ 175.2(5), $\text{C}(25)\text{--Rh}(1)\text{--P}(1)$ 91.6(2), $\text{C}(25)\text{--Rh}(1)\text{--Cl}(1)$ 174.2(2), $\text{P}(1)\text{--Rh}(1)\text{--Cl}(1)$ 87.7(4).

o-MeP with the free, gas-phase conformation (151°). Steric demands for free and co-ordinated phosphanes are shown in table 2.

As is characteristic of the *trans*- $\text{Rh}(\text{CO})\text{ClP}_2$ species, complex **9** (figure 3) shows disorder along the CO/Cl axis. Other interatomic bond distances and angles are comparable to analogous Vaska-type compounds [16,17]. Compared with structure **6**, the more bulky *o*-Et₂P ligand faces more steric repulsion, resulting in a lower cone angle in bonded state (178°) compared to the free gas-phase conformation (194°). However, in solid state the size of the ligand remains the same for free and bonded form.

2.5. Catalytic studies

Hydroformylation tests were conducted under 15 bar of syngas ($\text{CO}/\text{H}_2 = 1$) at temperatures of 80 and 120 $^\circ\text{C}$. $\text{Rh}_4(\text{CO})_{12}$ was used as a catalyst precursor *in situ* with added alkyl-substituted phosphanes at ligand to rhodium ratio of 10. The effect of the ligands on 1-hexene hydroformylation can be seen from tables 3 and 4.

All the catalyst systems afforded rather low chemoselectivity to aldehydes, with large amounts of the isomerization products, 2-hexene and even 3-hexene formed instead. Hydrogenation was not observed, however. High isomerization activity was, at least partly, a consequence of the rather mild reaction conditions applied (due to high activity of the $\text{Rh}_4(\text{CO})_{12}$) to reveal the differences between the ligands.

At 80 $^\circ\text{C}$ (table 3) only *o*-MeP gave conversion and total aldehyde yield comparable to the PPh_3 -modified reac-

tion. Any higher degree of substitution hindered the reaction, causing a drop in 1-hexene conversion. In fact, the conversion was dependent on cone angle, with the exception of *o*-Me₂P and 2,4,5-MeP ligands. Conversion was surprisingly low for *o*-Me₂P and even zero when 2,4,5-MeP was applied. The number and size of the alkyl groups also affect regioselectivity; relative to PPh_3 , the normal to branched ratio increases with methyl substituents and further with the use of ethyl groups in *ortho* position(s).

At elevated temperature (120 $^\circ\text{C}$) (table 4) the conversion levels were roughly the same with all the ligands. As for *o*-Me₂P the conversion was still lower compared to sterically more demanding *o*-EtP. Although, not representative for actual catalyst species, a similar setup as in complex **9** where both sides of the metal center are crowded with the alkyl substituents takes place also with *o*-Me₂P, thus hindering the reaction. Further, it turned out that the increase in temperature restored the activity of 2,4,5-MeP. The poor solubility is the probable reason for inactivity at lower temperature. The formation of the branched aldehydes increases at 120 $^\circ\text{C}$, as small amounts of 2-ethylpental are formed. However, the selectivity towards 1-heptanal decreases, except in the case of PPh_3 and *o*-MeP. The most sterically demanding ligand in the series, *o*-Et₂P, was observed to give the lowest *n/i* ratio. Owing to its bulkiness it is susceptible to dissociation during the catalytic cycle, thus increasing the coordinative unsaturation of rhodium and the formation of $\text{HRh}(\text{CO})_3(\text{L})$ species [1]. Such species are known to favor the formation of branched aldehydes, but also the hydroformylation activity

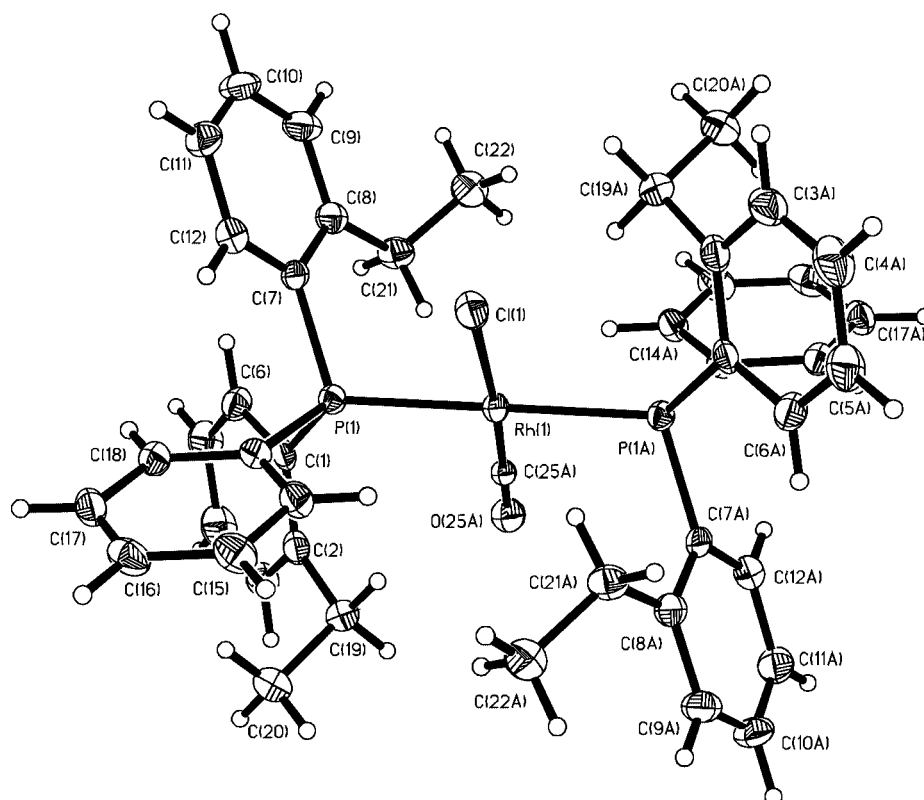


Figure 3. Ortep drawing of $\text{Rh}(\text{CO})\text{Cl}(\text{o-Et}_2\text{P})_2$ (**9**) with thermal ellipsoids at 50% level. Selected bond angles ($^\circ$) and distances (\AA): $\text{Rh}(1)\text{--C}(25)$ 1.728(8), $\text{Rh}(1)\text{--Cl}(1)$ 2.402(3), $\text{Rh}(1)\text{--P}(1)$ 2.332(8), $\text{Rh}(1)\text{--P}(1\text{B})$ 2.332(8), $\text{P}(1\text{B})\text{--Rh}(1)\text{--P}(1)$ 180.0(1), $\text{C}(25)\text{--Rh}(1)\text{--P}(1)$ 88.9(2), $\text{C}(25)\text{--Rh}(1)\text{--Cl}(1)$ 3.8(2), $\text{P}(1)\text{--Rh}(1)\text{--Cl}(1)$ 85.2(5).

Table 3
Effect of ligand on 1-hexene hydroformylation ($T = 80\text{ }^\circ\text{C}$).^a

Ligand	Cone angle	Conversion (%)	<i>S</i> (isomers) (%)	<i>S</i> (2Mh) (%)	<i>S</i> (h) (%)	<i>n/i</i>
PPh_3	149°	79	89	4	8	2.2
<i>o</i> -MeP	151°	75	89	3	8	2.4
<i>o</i> -EtP	169°	13	84	3	9	2.8
<i>o</i> -Et ₂ P	194°	10	90	3	7	2.7
<i>o</i> -Me ₂ P	158°	5	90	3	7	2.6
2,4,5-MeP	159°	0	0	0	0	–

^a Reaction conditions: 15 bar ($\text{CO}/\text{H}_2 = 1$), 2 h, 1-hexene 15.5 mmol, toluene 5 ml, $\text{Rh}_4(\text{CO})_{12}$ 1.9×10^{-2} mmol, $\text{L}/\text{Rh} = 10$. *S*(isomers) = total amount of 2- and 3-hexenes; *S*(2Mh) = selectivity to 2-methylhexanal; *S*(h) = selectivity to 1-heptanal.

Table 4
Effect of ligand on 1-hexene hydroformylation ($T = 120\text{ }^\circ\text{C}$).^a

Ligand	Cone angle	Conversion (%)	<i>S</i> (isomers) (%)	<i>S</i> (2Ep) (%)	<i>S</i> (2Mh) (%)	<i>S</i> (h) (%)	<i>n/i</i>
<i>o</i> -MeP	151°	85	84	2	7	8	0.9
<i>o</i> -EtP	169°	82	91	1	3	4	1.1
PPh_3	149°	82	84	2	7	8	0.9
2,4,5-MeP	159°	80	91	1	4	4	0.9
<i>o</i> -Me ₂ P	158°	80	91	1	4	4	0.9
<i>o</i> -Et ₂ P	194°	76	90	2	5	4	0.7

^a Reaction conditions: 15 bar ($\text{CO}/\text{H}_2 = 1$), 2 h, 1-hexene 15.5 mmol, toluene 5 ml, $\text{Rh}_4(\text{CO})_{12}$ 1.9×10^{-2} mmol, $\text{L}/\text{Rh} = 10$. *S*(2Ep) = selectivity to 2-ethylpentanal.

due to highly carbonylated rhodium species. Indeed, *o*-Et₂P gave comparatively high total aldehyde selectivity, and only the PPh_3 - and *o*-MeP-modified systems gave higher selectivity. The lower regioselectivity to normal products could also be attributed to the basicity of the ligand, as more basic phosphanes are reported to yield lower *n/i* ratios [8,11]. On the other hand, basic phosphanes are also known to enhance the formation of more carbonylated species [19], thus making it difficult to separate and quantify the steric and electronic effects.

3. Conclusions

Efforts were made to clarify the electron donor/acceptor properties of the ligands with the aid of spectroscopic data of the co-ordination compounds. However, the variation in size, position, and amount of alkyl group had only minor effects on the electronic character of the ligand, as demonstrated by the similarity of the $\nu(\text{CO})$ and $^1J_{\text{Rh-P}}$ values.

The size of the ligand had an effect on the 1-hexene hydroformylation results, however. The conversion was negatively affected with increasing steric demands of the ligands. Furthermore, the smallest ligand in the series, *o*-MeP gave an aldehyde yield and *n/i* ratio comparable to that of PPh_3 . In contrast, the ligand with largest bulk, *o*-Et₂P, favored the formation of branched aldehydes, most probably due to the formation of $\text{HRh}(\text{CO})_3(\text{L})$ species.

Acknowledgement

Financial support was provided by Neste Chemicals Oy.

Appendix: Experimental

A.1. Ligands

A.1.1. General comments

All alkyl-substituted ligands were prepared by a modified literature method, where lithiated compounds were used instead of Grignard reagents [20]. Commercially available reagents were used without further purification. Diethyl ether (Lab Scan) was distilled from sodium/benzophenone ketyl under nitrogen before use. All ligand syntheses were carried out with standard Schlenk techniques under nitrogen or argon atmosphere.

A.1.2. Spectroscopy

The characterization of the ligands was based mainly on ^1H , $^{13}\text{C}\{^1\text{H}\}$, and $^{31}\text{P}\{^1\text{H}\}$ NMR spectroscopy. NMR spectra were recorded on Bruker AM200 and DPX400 spectrometers at room temperature in CDCl_3 . ^1H NMR: reference SiMe_4 . $^{13}\text{C}\{^1\text{H}\}$ NMR: CDCl_3 set to 77.0 ppm. $^{31}\text{P}\{^1\text{H}\}$ NMR: external standard 85% H_3PO_4 . Two-dimensional HSQC NMR spectra were also measured and in the case of 2,4,5-MeP, a noesy-experiment was needed to resolve the shifts of the methyl substituents. Exact mass peaks were determined on a Micromass LCT, ESI+.

A.1.3. Synthesis and characterisation

(2,4,5-trimethylphenyl)diphenylphosphane (2,4,5-MeP). When a solution of *n*-butyllithium (22.8 ml, 57 mmol, Aldrich, 2.5 M solution in hexane) was added dropwise at $-10 \rightarrow 0^\circ\text{C}$ (salted ice bath) to a solution of 5-bromo-2,2,4-trimethylbenzene (5.77 g, 29 mmol, Aldrich, 99%) in diethyl ether (50 ml), the reaction mixture turned yellow and eventually white. The mixture was stirred for 2 h at this temperature. Addition of a solution of chlorodiphenylphosphane (6.40 g, 29 mmol, Aldrich, 95%) in diethyl ether (20 ml) colored the reaction mixture orange. The mixture was stirred at $-10 \rightarrow 0^\circ\text{C}$ for a further 2 h. After slow warming to room temperature, some solid material precipitated (inorganic salts). The mixture was filtrated and the solvent was removed *in vacuo*. The product was recrystallized from ethanol. The yield of the product was 5.66 g, 18.6 mmol, 64.1%. ^1H NMR (400 MHz, CDCl_3): δ 2.04 (s, 3 H, H^{13}), 2.20 (s, 3 H, H^{12}), 2.33 (s, 3 H, H^{11}), 6.54 (d, $^3J_{\text{H-H}} = 4.8$ Hz, 1 H, H^6), 6.98 (d, $^4J_{\text{H-P}} = 4.8$ Hz, 1 H, H^3), 7.29 (broad singlet, 10 H, H^8 , H^9 and H^{10}). $^{13}\text{C}\{^1\text{H}\}$ NMR (100 MHz, CDCl_3): δ 19.19 (s, 1 C, C^{13}), 19.32 (s, 1 C, C^{12}), 20.47 (d, $^3J_{\text{C-P}} = 20.5$ Hz, 1 C, C^{11}), 128.33 (d, $^3J_{\text{C-P}} = 6.8$ Hz, 4 C, C^9), 128.45 (s, 2 C, C^{10}), 128.00–129.00 (2 C, C^4 and C^5), 131.50 (d, $^3J_{\text{C-P}} = 4.9$ Hz, 1 C, C^3), 133.75 (d, $^2J_{\text{C-P}} = 19.6$ Hz, 4 C, C^8), 133.87 (s, 1 C, C^6), 136.52 (d, $^1J_{\text{C-P}} = 10.3$ Hz, 1 C, C^1), 137.19 (s, 2 C, C^7), 139.50 (d, $^2J_{\text{C-P}} = 25.4$ Hz, 1 C, C^2). $^{31}\text{P}\{^1\text{H}\}$ NMR

(161 MHz, CDCl_3): δ -12.9. TOF MS ES+ calcd for $(\text{M} + \text{H})^+$ ($\text{C}_{21}\text{H}_{22}\text{P}$) 305.1459, found 305.1448.

Since the previous literature [20–23] does not contain detailed NMR spectra for these compounds, the resolved ^1H and $^{13}\text{C}\{^1\text{H}\}$ NMR spectra are presented here, as well as the $^{31}\text{P}\{^1\text{H}\}$ chemical shifts.

(*o*-methylphenyl)diphenylphosphane (*o*-MeP): yield 53.2%. ^1H NMR (200 MHz, CDCl_3): δ 2.39 (s, 3 H, H^{11}), 6.76 (dd, $^3J_{\text{H-H}} = 7.4$ Hz, $^3J_{\text{H-P}} = 4.5$ Hz, 1 H, H^6), 7.08 (td, $^3J_{\text{H-H}} = 7.0$ Hz, $^4J_{\text{H-P}} = 2.1$ Hz, 1 H, H^5), 7.20–7.37 (m, 12 H, H^3 , H^4 , H^8 , H^9 and H^{10}). $^{13}\text{C}\{^1\text{H}\}$ NMR (100 MHz, CDCl_3): δ 21.18 (d, $^3J_{\text{C-P}} = 20.9$ Hz, 1 C, C^{11}), 125.97 (s, 1 C, C^5), 128.52 (d, $^3J_{\text{C-P}} = 6.3$ Hz, 4 C, C^9), 128.55 (s, 1 C, C^4), 128.71 (s, 2 C, C^{10}), 130.03 (d, $^3J_{\text{C-P}} = 3.5$ Hz, 1 C, C^3), 132.70 (s, 1 C, C^6), 133.98 (d, $^2J_{\text{C-P}} = 19.0$ Hz, 4 C, C^8), 135.95 (d, $^1J_{\text{C-P}} = 11.7$ Hz, 1 C, C^1), 136.25 (d, $^1J_{\text{C-P}} = 10.0$ Hz, 2 C, C^7), 142.17 (d, $^2J_{\text{C-P}} = 25.3$ Hz, 1 C, C^2). $^{31}\text{P}\{^1\text{H}\}$ NMR (161 MHz, CDCl_3): δ -12.1.

(*o*-ethylphenyl)diphenylphosphane (*o*-EtP): yield 50.2%. ^1H NMR (200 MHz, CDCl_3): δ 1.16 (t, $^3J_{\text{H-H}} = 7.6$ Hz, 3 H, H^{12}), 2.87 (qd, $^3J_{\text{H-H}} = 7.5$ Hz, $^4J_{\text{H-P}} = 1.6$ Hz, 2 H, H^{11}), 6.83 (dd, $^3J_{\text{H-H}} = 7.6$ Hz, $^3J_{\text{H-P}} = 4.2$ Hz, 1 H, H^6), 7.09 (td, $^3J_{\text{H-H}} = 7.6$ Hz, $^4J_{\text{H-P}} = 2.5$ Hz, 1 H, H^5), 7.21–7.36 (m, 12 H, H^3 , H^4 , H^8 , H^9 and H^{10}). $^{13}\text{C}\{^1\text{H}\}$ NMR (100 MHz, CDCl_3): δ 15.29 (s, 1 C, C^{12}), 27.35 (d, $^3J_{\text{C-P}} = 22.2$ Hz, 1 C, C^{11}), 125.95 (s, 1 C, C^5), 128.20 (s, 1 C, C^4), 128.41 (d, $^3J_{\text{C-P}} = 6.3$ Hz, 4 C, C^9), 128.52 (s, 2 C, C^{10}), 129.00 (s, 1 C, C^3), 133.38 (s, 1 C, C^6), 133.82 (d, $^2J_{\text{C-P}} = 19.7$ Hz, 4 C, C^8), 135.05 (d, $^1J_{\text{C-P}} = 11.9$ Hz, 1 C, C^1), 136.94 (d, $^1J_{\text{C-P}} = 10.4$ Hz, 2 C, C^7), 148.54 (d, $^2J_{\text{C-P}} = 25.1$ Hz, 1 C, C^2). $^{31}\text{P}\{^1\text{H}\}$ NMR (161 MHz, CDCl_3): δ -14.0.

Bis(*o*-methylphenyl)phenylphosphane (*o*-Me₂P): yield 87.2%. ^1H NMR (200 MHz, CDCl_3): δ 2.39 (s, 6 H, H^{11}), 6.73 (dd, $^3J_{\text{H-H}} = 7.7$ Hz, $^3J_{\text{H-P}} = 4.3$ Hz, 2 H, H^6), 7.08 (td, $^3J_{\text{H-H}} = 7.6$ Hz, $^4J_{\text{H-P}} = 2.4$ Hz, 2 H, H^5), 7.20–7.38 (m, 9 H, H^3 , H^4 , H^8 , H^9 and H^{10}). $^{13}\text{C}\{^1\text{H}\}$ NMR (100 MHz, CDCl_3): δ 21.16 (d, $^3J_{\text{C-P}} = 20.7$ Hz, 2 C, C^{11}), 126.05 (s, 2 C, C^5), 128.55 (d, 2 C, C^9), 128.64 (s, 1 C, C^4), 128.75 (s, 1 C, C^{10}), 130.04 (d, $^3J_{\text{C-P}} = 4.8$ Hz, 2 C, C^3), 132.85 (s, 2 C, C^6), 134.32 (d, $^2J_{\text{C-P}} = 20.7$ Hz, 2 C, C^8), 135.19 (d, $^1J_{\text{C-P}} = 11.1$ Hz, 2 C, C^1), 135.47 (d, $^1J_{\text{C-P}} = 9.5$ Hz, 1 C, C^7), 142.40 (d, $^2J_{\text{C-P}} = 25.4$ Hz, 2 C, C^2). $^{31}\text{P}\{^1\text{H}\}$ NMR (161 MHz, CDCl_3): δ -19.0.

Bis(*o*-ethylphenyl)phenylphosphane (*o*-Et₂P): yield 70.5%. ^1H NMR (200 MHz, CDCl_3): δ 1.15 (t, $^3J_{\text{H-H}} = 7.5$ Hz, 6 H, H^{12}), 2.84 (qd, $^3J_{\text{H-H}} = 7.6$ Hz, $^4J_{\text{H-P}} = 1.4$ Hz, 4 H, H^{11}), 6.78 (dd, $^3J_{\text{H-H}} = 7.4$ Hz, $^3J_{\text{H-P}} = 4.4$ Hz, 2 H, H^6), 7.08 (td, $^3J_{\text{H-H}} = 7.0$ Hz, $^4J_{\text{H-P}} = 2.5$ Hz, 2 H, H^5), 7.20–7.35 (m, 9 H, H^3 , H^4 , H^8 , H^9 and H^{10}). $^{13}\text{C}\{^1\text{H}\}$ NMR (100 MHz, CDCl_3): δ 15.15 (s, 2 C, C^{12}), 27.43 (d, $^3J_{\text{C-P}} = 22.3$ Hz, 2 C, C^{11}), 125.97 (s, 2 C, C^5), 128.21 (d, $^3J_{\text{C-P}} = 4.8$ Hz, 2 C, C^9), 128.42 (s, 1 C, C^{10}), 128.50 (s, 2 C, C^4), 128.94 (s, 2 C, C^3), 133.64 (s, 2 C, C^6), 134.16 (d, $^2J_{\text{C-P}} = 20.7$ Hz, 2 C, C^8), 135.05 (d, $^1J_{\text{C-P}} = 11.1$ Hz, 2 C, C^1), 136.82 (d, $^1J_{\text{C-P}} = 11.1$ Hz, 1 C, C^7), 148.50

(d, $^2J_{C-P} = 25.4$ Hz, 2 C, C²). $^{31}P\{^1H\}$ NMR (161 MHz, CDCl₃): δ -23.5.

A.2. X-ray crystallography

X-ray diffraction data were collected with a Nonius KappaCCD diffractometer using Mo K α radiation ($\lambda = 0.71073$ Å) and ϕ -scan data collection mode with the Collect [24] collection program. Denzo and Scalepack [25] programs were used for cell refinements and data reduction. All structures were solved by direct methods using the SIR97 [26] program and the WinGX [27] graphical user interface. Structure refinements were carried out with the SHELXL97 [28] program. Crystallographic data (excluding structure factors) for the structures **2**, **3**, **4**, **6**, and **9** have been deposited with the Cambridge Crystallographic Data Centre as supplementary publication no. CCDC 159190-159194. Copies of the data can be obtained free of charge on application to CCDC, 12 Union Road, Cambridge CB2 1EZ, UK (fax: int. code + 44(1223)336-033; e-mail: deposit@ccdc.cam.ac.uk).

A.3. Hydroformylation experiments

1-hexene hydroformylation reactions were conducted in a 100 ml autoclave (Berghof) with 60 ml Teflon liner. The experiments were done in batch mode with rhodium precursor Rh₄(CO)₁₂, which was prepared according to literature method [29]. The reactor was charged under a nitrogen purge with substrate, rhodium catalyst, ligand (L/Rh = 10), and internal standard, cyclohexane. The autoclave was then sealed and pressurized using a 1 : 1 mixture of H₂ and CO (MG, 99.997%) to 15 bar and heated to 80 or 120 °C. After 2 h, the autoclave was cooled and brought to normal atmospheric pressure. The reproducibility of the test system was confirmed by doing each test twice.

A disposable inner Teflon reactor was used to avoid accumulation of rhodium on the reactor walls. In addition, before each experiment the purity of the system was checked with blank runs. The products were analyzed with a Hewlett-Packard 5890 GC equipped with a capillary column (HP-1, 1.0 μ m \times 0.32 mm \times 60 m) and a flame-ionization detector. Products were quantified by the internal standard method. In addition, the aldehydes that formed were identified by GC-MS analysis.

Calculations of conversion, selectivity, and *i/n* ratio were done on molar basis. Conversion was calculated with respect to 1-hexene. The *i/n* ratio of the aldehydes was defined as the amount of branched product divided by the amount of linear product.

References

- [1] B. Cornils and W.A. Herrmann, *Applied Homogeneous Catalysis with Organometallic Compounds*, Vol. 1 (VCH, Weinheim, 1996).
- [2] M. Beller, B. Cornils, C.D. Frohning and C.W. Kohlpaintner, *J. Mol. Catal.* 104 (1995) 17.
- [3] P.C.J. Kamer, J.N.H. Reek and P.W.N.M. van Leeuwen, *Chemtech* (1998) 27.
- [4] C.A. Tolman, *Chem. Rev.* 77 (1977) 313.
- [5] C.P. Casey, G.T. Whiteker, M.G. Melville, L.M. Petrovich, J.A. Gavney Jr. and D.R. Powell, *J. Am. Chem. Soc.* 114 (1992) 5535.
- [6] C.A. Tolman, *J. Am. Chem. Soc.* (1970) 2953.
- [7] G.M. Bancroft, L. Dignard-Bailey and R. Puddephatt, *J. Inorg. Chem.* 25 (1986) 3675.
- [8] C.A. Streuli, *Anal. Chem.* 32 (1960) 985; 31 (1959) 1652.
- [9] W. Leitner, M. Bühl, R. Fornika, C. Six, W. Baumann, E. Dinjus, M. Kessler, C. Krüger and A. Rufinska, *Organometallics* 18 (1999) 1196.
- [10] S. Montetatici, A. van der Ent, J.A. Osborn and G. Wilkinson, *J. Chem. Soc. A* (1968) 1054.
- [11] W.R. Moser, C.J. Papile, D.A. Brannon, R.A. Duwell and S.J. Weininger, *J. Mol. Catal.* 41 (1987) 271.
- [12] H.K. Reinius, P. Suomalainen, H. Riihimäki, E. Karvinen, J. Pursiainen and A.O.I. Krause, *J. Catal.* 199 (2001) 302.
- [13] D.W. Meek, G. Dryer and M.O. Workman, *Inorg. Synth.* 16 (1976) 168.
- [14] J.F. Nixon and A. Pidcock, *Annu. Rev. NMR Spectrosc.* 2 (1969) 345.
- [15] M.R. Wilson, D.C. Woska, A. Prock and W.P. Giering, *Organometallics* 12 (1993) 1742.
- [16] F.R. Hartley, S.G. Murray and D.M. Potter, *J. Organomet. Chem.* 254 (1983) 119.
- [17] S. Otto, S.N. Mzamane and A. Roodt, *Acta Cryst. C* 55 (1999) 67.
- [18] J.D. Unruh and J.R. Christenson, *J. Mol. Catal.* 14 (1982) 19.
- [19] O.R. Hughes and D.A. Young, *J. Am. Chem. Soc.* 103 (1981) 6636.
- [20] L. Horner and G. Simons, *Phosphorus and Sulfur* 14 (1983) 189.
- [21] D.W. Allen, *Z. Naturforsch.* 35B 11 (1980) 1455.
- [22] M. Culcasi, Y. Berchadsky, G. Gronchi and P. Tordo, *J. Org. Chem.* 56 (1991) 3537.
- [23] J.F. Blount, D. Camp, R.D. Hart, P.C. Healy, B.W. Skelton and A.H. White, *Aust. J. Chem.* 47 (1994) 1631.
- [24] *Collect* data collection software, Nonius (1999).
- [25] Z. Otwinowski and W. Minor, in: *Methods in Enzymology*, Vol. 276, Macromolecular Crystallography, part A, eds. C.W. Carter Jr. and R.M. Sweet (Academic Press, New York, 1997) pp. 307–326.
- [26] A. Altomare, M.C. Burla, M. Camalli, G.L. Cascarano, C. Giacovazzo, A. Guagliardi, A.G.G. Moliterni, G. Polidori and R.J. Spagna, *J. Appl. Cryst.* 32 (1999) 115–119.
- [27] L.J. Farrugia, *J. Appl. Cryst.* 32 (1999) 837–838.
- [28] G.M. Sheldrick, SHELXL97, Program for Crystal Structure Refinement, University of Göttingen (1997).
- [29] S. Martinengo, G. Giordano and P. Chini, *Inorganic Syntheses*, Vol. 20 (Wiley, New York, 1980) p. 209.